

Inapplicability of exact constraints and a minimal two-parameter generalization to the DFT+ U based correction of self-interaction error

Glenn Moynihan,^{1,*} Gilberto Teobaldi,^{2,3} and David D. O'Regan¹

¹*School of Physics, CRANN and AMBER, Trinity College Dublin, Dublin 2, Ireland*

²*Stephenson Institute for Renewable Energy and Department of Chemistry,
The University of Liverpool, L69 3BX Liverpool, United Kingdom*

³*Beijing Computational Science Research Center, Beijing 100094, China*

(Dated: December 15, 2016)

In approximate density functional theory (DFT), the self-interaction error is an electron delocalization anomaly associated with underestimated insulating gaps. It exhibits a predominantly quadratic energy-density curve that is amenable to correction using efficient, constraint-resembling methods such as DFT + Hubbard U (DFT+ U). Constrained DFT (cDFT) enforces conditions on DFT exactly, by means of self-consistently optimized Lagrange multipliers, and while its use to automate error corrections is a compelling possibility, we show that it is limited by a fundamental incompatibility with constraints beyond linear order. We circumvent this problem by utilizing separate linear and quadratic correction terms, which may be interpreted either as distinct constraints, each with its own Hubbard U type Lagrange multiplier, or as the components of a generalized DFT+ U functional. The latter approach prevails in our tests on a model one-electron system, H_2^+ , in that it readily recovers the exact total-energy while symmetry-preserving pure constraints fail to do so. The generalized DFT+ U functional moreover enables the simultaneous correction of the total-energy and ionization potential, or the correction of either together with the enforcement of Koopmans' condition. For the latter case, we outline a practical, approximate scheme by which the required pair of Hubbard parameters, denoted as U_1 and U_2 , may be calculated from first-principles.

PACS numbers: 71.15.-m, 31.15.E-, 71.15.Qe, 71.15.Dx

Approximate density-functional theory (DFT)^{1,2} underlies much of contemporary quantum-mechanical atomistic simulation, providing a widespread and valuable complement to experiment^{3,4}. The predictive capacity of DFT is severely limited, however, by systematic errors⁵⁻⁷ exhibited by tractable exchange-correlation functionals such as the local-density approximation (LDA)⁸ or generalized-gradient approximations⁹. Perhaps the most prominent of these pathologies is the delocalization or many-electron self-interaction error (SIE)⁸, which is due to spuriously curved rather than correctly piecewise-linear total-energy profiles with respect to the total electron number^{5,6}. This gives rise to the underestimated fundamental gaps⁵, charge-transfer energies¹⁰, and reaction barriers¹¹ characteristic of practical DFT. While the construction of viable, explicit density functionals free of pathologies such as SIE is extremely challenging¹², significant progress has been made in the development of implicit functionals in the guise of corrective approaches. Examples include methods that operate by correcting SIE on a one-electron basis according to variationally optimized definitions, such as generalized¹³⁻¹⁵ Perdew-Zunger⁸ approaches, in which much progress has recently been made by generalizing to complex-valued orbitals¹⁶⁻¹⁸, and those which address many-electron SIE directly, such as Koopman's compliant functionals^{7,19}.

An established, computationally very efficient DFT correction scheme is DFT+ U ²⁰⁻²⁵, originally developed to restore the Mott-Hubbard effects absent in the LDA description of transition-metal oxides. A simplified formulation²³⁻²⁵, in which the required Hubbard U param-

eter is a linear-response property of the system under scrutiny²⁵, is now routinely and diversely applied²⁶⁻³⁰. Beginning with Ref. 11, Marzari, Kulik, and co-workers have suggested and extensively developed^{31,32} the interpretation of DFT+ U as a correction for SIE, for systems in which it may be primarily attributed to distinct subspaces (otherwise, the related Koopman's compliant functionals are available^{7,19}). The SIE correcting DFT+ U functional is given, where $\hat{n}^{I\sigma} = \hat{P}^I \hat{\rho}^\sigma \hat{P}^I$, by

$$E_U = \sum_{I\sigma} \frac{U^I}{2} \text{Tr} [\hat{n}^{I\sigma} - \hat{n}^{I\sigma} \hat{n}^{I\sigma}]. \quad (1)$$

Here, $\hat{\rho}^\sigma$ is the Kohn-Sham density-matrix for spin σ and \hat{P}^I is a projection operator for the subspace I . DFT+ U attains the status of an automatable, first-principles method when it is provided with calculated Hubbard U parameters^{24,25,28,33,34} (particularly at their self-consistency^{11,30,35}), which may be thought of as subspace-averaged SIEs quantified in situ. The subspaces are usually pre-defined for corrective treatment, having been deemed responsible for the dominant SIEs on the basis of physical intuition and experience, although a further level of self-consistency over subspaces is possible using Wannier functions³⁶. DFT+ U effectively adds a set of penalty functionals promoting integer eigenvalues in $\hat{n}^{I\sigma}$, and it replicates the effect of a derivative discontinuity in the energy, for each subspace I , by adding an occupancy-dependent potential $\hat{v}^{I\sigma} = U^I(\hat{P}^I/2 - \hat{n}^{I\sigma})$.

While DFT+ U is effective and computationally efficient, even linear-scaling³⁷, a considerable degree of care is needed to calculate the required U parameters, which

sometimes pose numerical challenges^{28,31}. Fully self-contained calculations of the Hubbard U by means of automated variational extremization would be extremely useful for many practitioners, and expedient in high-throughput materials search contexts³⁸. The constraint-like functional form of DFT+ U , where the U^I resemble the Lagrange multipliers of penalty functionals on the eigenvalues of $\hat{n}^{I\sigma}$, suggests the possible viability of such a method. Constrained density-functional theory (cDFT)^{10,39,40} formalizes and automates the use of self-consistent⁴¹ penalty functionals in DFT, enforcing them as exact constraints by locating the lowest-energy compatible excited state of the underlying functional. It is effective for treating SIE, in its own right, for systems comprising well-separated fragments, where it may be used to break physical symmetries and to explore the integer-occupancy states at which SIE is typically reduced^{10,42}. However, as we now demonstrate, cDFT is fundamentally incompatible with constraints beyond linear order, and therefore exact constraints cannot be used to correct SIE in an automated fashion. As a result, it seems that we cannot excite a SIE affected system to a state that will reliably exhibit less SIE, without breaking a symmetry.

The simplest conceivable SIE-targeting constraint functional is the quadratic form $C_2 = \sum_I (N^I - N_c^I)^2$, where $N^I = \text{Tr}[\hat{n}^I]$ is the total occupancy of a particularly error-prone subspace I and N_c^I is its targeted value, neglecting the spin index for concision. This constraint is a functional of subspace total occupancies, rather than the occupancy eigenvalues as in DFT+ U , which is an important distinction for all but single-orbital sites. For N_{sites} symmetry-equivalent subspaces with $N_c^I = N_c$ for all I , the total-energy of the system is given by $W = E_{\text{DFT}} + V_c C_2$, where V_c is a common cDFT Lagrange multiplier. This gives rise to a constraining potential of the form $\hat{v}_c = 2V_c \sum_I (N^I - N_c) \hat{P}^I$, making explicit its dependence on the constraint non-satisfaction. This, in turn, implies an externally imposed interaction correction given by $\hat{f}_c = 2V_c \sum_I \hat{P}^I \hat{P}^I$, which acts to modify the energy-density profile, and which is identical to that generated by DFT+ U (Eq. 1) when $V_c = -U^I/2$.

Following Ref. 41 for the self-consistent cDFT problem, the Hellmann-Feynman theorem provides that the first energy derivative is simply the constraint functional, i.e., $dW/dV_c = C_n$, so that the total-energy $W(V_c)$ always attains a stationary point upon constraint satisfaction, in this case when $C_2 = 0$. Fig. 1 depicts this function for an ideal system for the study of one-electron SIE^{6,12}, H_2^+ , simulated⁴³ using the PBE functional⁹. At the considered, intermediate bond-length of 4 a_0 , the overlap of the two atom-centered PBE 1s orbital subspaces yields a total occupancy double-counting of 24%, accounting for spillage. The observed asymptotic behavior of $W(V_c)$ demonstrates that the C_2 constraint is unenforceable. Here, a target occupancy of $N_c = 0.5$ e has been applied, necessitating a repulsive constraint and a positive V_c , but the same qualitative outcome arises for any $N_c \neq N_{\text{DFT}}$.

The key to the failure of the C_2 constraint is the

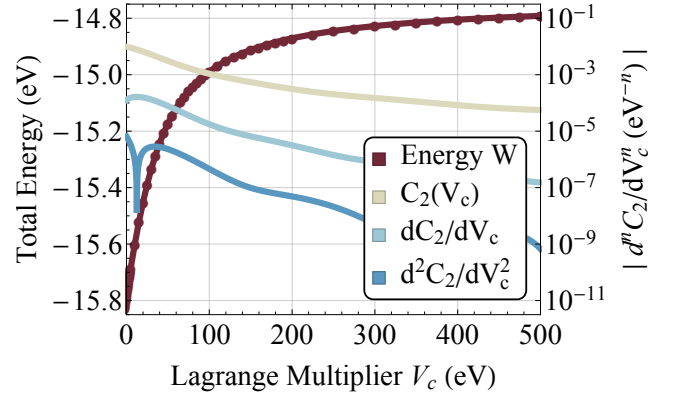


FIG. 1. (Color online) The constrained total-energy of the stretched H_2^+ system, with a target occupancy of $N_c = 0.5$ e per fixed atom-centered 1s-orbital subspace, against the cDFT Lagrange multiplier V_c . Also shown is the constraint functional $C_2 = (N - N_c)^2$, averaged over the two atoms, and its first and second derivatives, which all fall off rapidly with V_c .

fall-off of all self-consistent cDFT response functions⁴¹ $d^n N/dV_c^n = d^{n+1} W/dV_c^{n+1}$, as depicted in Fig. 2. This results in a diminishing returns as V_c is increased, i.e., as the constraint asymptotically approaches satisfaction. Motivated by this, we investigate whether non-linear constraints of form $C_n = (N - N_c)^n$ are unsatisfiable for any order $n \neq 1$ and for any target choice $N_c \neq N_{\text{DFT}}$. The $n = 0$ case is trivial, and the constraint is ill-defined for $n < 0$ since there the total-energy diverges upon constraint satisfaction. C_n becomes imaginary for non-integer n with negative $(N - N_c)$, so that we may limit our discussion to integers $n \geq 2$. We begin by analyzing the derivatives of the total-energy $W(V_c)$. The second derivative follows directly from the above discussion, as

$$\frac{d^2 W}{dV_c^2} = \frac{dC_n}{dV_c} = n(N - N_c)^{n-1} \frac{dN}{dV_c}. \quad (2)$$

The energy derivative of order m generally involves cDFT response functions up to order $m - 1$, and positive integer powers of $(N - N_c)$ which may vanish, depending on m and n , but not diverge. The cDFT response function dN/dV_c may be gainfully expanded, if \hat{v}_{ext} is the external potential, in terms of the intrinsic subspace-projected interacting response function defined by $\chi = \text{Tr}[(dN/d\hat{v}_{\text{ext}})\hat{P}]$, since this object is independent of the form of the constraint. The first-order cDFT response dN/dV_c is thus expressed, by means of the chain rule in $\hat{v}_{\text{ext}} = \hat{v}_c = V_c(\delta C_n/\delta \hat{\rho}) = nV_c(N - N_c)^{n-1} \hat{P}$, as

$$\begin{aligned} \frac{dN}{dV_c} &= \text{Tr} \left[\frac{dN}{d\hat{v}_{\text{ext}}} \frac{d\hat{v}_{\text{ext}}}{dV_c} \right] = n\chi \frac{d}{dV_c} [V_c C_{n-1}] \\ \Rightarrow \frac{dN}{dV_c} &= n\chi C_{n-1} \left(1 - n(n-1)\chi V_c C_{n-2} \right)^{-1}, \quad (3) \end{aligned}$$

an expression which we have verified numerically. At any valid stationary point, $C_n = 0$ and each of V_c , χ , and its

derivatives must remain finite. Thus, for $n \geq 2$, the response dN/dV_c and energy curvature d^2W/dV_c^2 both then vanish. The latter is therefore not a stationary point discriminant, and we move to higher derivatives, such as

$$\frac{d^3W}{dV_c^3} = n(n-1)C_{n-2} \left(\frac{dN}{dV_c} \right)^2 + nC_{n-1} \frac{d^2N}{dV_c^2}, \quad (4)$$

where the required second-order response is given by

$$\begin{aligned} \frac{d^2N}{dV_c^2} = & n \left[\frac{d\chi}{dV_c} C_{n-1} + (n-1) \frac{dN}{dV_c} \right. \\ & \times \left(\frac{d\chi}{dV_c} V_c C_{n-2} + 2\chi C_{n-2} \right. \\ & \left. \left. + (n-2)\chi V_c C_{\max(n-3,0)} \frac{dN}{dV_c} \right) \right] \\ & \times \left(1 - n(n-1)\chi V_c C_{n-2} \right)^{-1}. \end{aligned} \quad (5)$$

This object, and thus d^3W/dV_c^3 both vanish at stationary points for all $n \geq 2$, due to the vanishing C_{n-1} in the first term of Eq. 5, and due to the vanishing first-order response (for which, see Eq. 3) in all remaining terms.

In general, the cDFT response function d^mN/dV_c^m comprises terms proportional to response functions of the same type but of lower order, plus a single term which is proportional to a potentially non-vanishing mixed response function $d^{m-1}\chi/dV_c^{m-1}$ multiplied by the necessarily vanishing C_{n-1} . This serves as an inductive proof that response functions at all orders, beginning with dN/dV_c , vanish as we approach a vanishing C_n , as illustrated in Fig. 2. Then, since each term in the m^{th} energy derivative is always proportional to non-divergent powers of $(N - N_c)$ and response functions of at most order $m-1$, all energy derivatives tend to zero, as depicted in Fig. 1, proving the conjecture. Thus, non-linear constraints of SIE-targeting C_n form cannot be enforced.

In order to cast the SIE-targeting C_n functional into a viable form, one possible option remains. We may expand the single-site C_2 , for example, as $C_2 = -2N_c V_c (N - N_c) - V_c (N_c^2 - N^2)$, and afford an additional degree of freedom to the system by decoupling these two terms. Writing the result in the notation of DFT+ U , by change of variables, we arrive at the constraint energy

$$\sum_I \frac{U_1}{2} (N^I - N_c) + \sum_I \frac{U_2}{2} (N_c^2 - N^{I2}). \quad (6)$$

The vanishing response problem is now circumvented, by interpreting the Hubbard U parameters for linear and quadratic terms as separate Lagrange multipliers. Adapting Eq. 6 to multiple, multi-orbital sites and neglecting inter-eigenvalue terms, in the spirit of DFT+ U , while retaining only the free-energy⁴⁴ (setting $N_c^I = 0$), we arrive at the generalized DFT+ U correction given by

$$E_{U_1 U_2} = \sum_{I\sigma} \frac{U_1^I}{2} \text{Tr} [\hat{n}^{I\sigma}] - \sum_{I\sigma} \frac{U_2^I}{2} \text{Tr} [\hat{n}^{I\sigma 2}]. \quad (7)$$

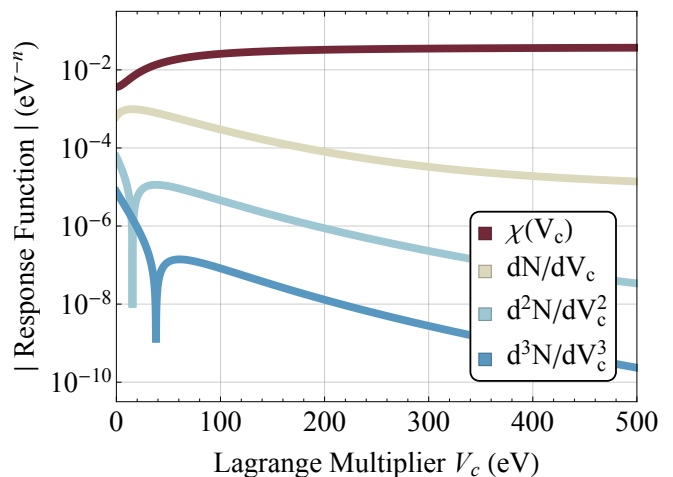


FIG. 2. (Color online) The magnitudes of the interacting density response χ and cDFT response functions d^mN/dV_c^m , calculated from a polynomial fit to the average subspace occupancy for the same system as in Fig. 1. The d^mN/dV_c^m fall off as we asymptotically approach constraint satisfaction, while the occupancy, and hence χ , tends to a constant value.

Here, the DFT+ U functional of Eq. 1 is recovered by setting $U_1^I = U_2^I$. Otherwise, the corrective potential is modified to $\hat{v}_{U_1 U_2}^I = U_1^I \hat{P}/2 - U_2^I \hat{n}^I$, so that the characteristic occupancy eigenvalue dividing an attractive from a repulsive potential is changed from $1/2$ to $U_1^I/2U_2^I$. Self-consistency effects aside, the U_2 parameters are responsible for correcting the interaction and for any gap modification, while the U_1 parameters may be used to adjust the linear dependence of the energy on the subspace occupancies, and thereby to refine eigenvalue derived properties such as the ionization potential. We note a resemblance between Eq. 7 and the three-parameter DFT+ $U\alpha\beta$ functional proposed in Ref. 45, where here a third degree of freedom may be retained by using $N_c^I \neq 0$.

Fig. 3 shows the total-energy W of the H_2^+ system as before, but now against the U_1 and U_2 defined in Eq. 6, with a subspace target occupancy of $N_c = N_{\text{exact}} = 0.602$ e, (the population of each of the two PBE $1s$ orbital subspaces, calculated using the exact functional). The total-energy is non-uniquely maximized along the heavy white line where the constraint is satisfied, at ~ 0.92 eV below the exact energy. To understand why the total-energy is always degenerate, and hence why the occupancy condition under-defines the pair (U_1, U_2) , it suffices to show that the Hessian of the constraint functional, $H_{ij} = d^2W/dU_i dU_j$ ⁴⁶, is everywhere singular. The determinant of H_{ij} is conveniently calculated in terms of the response functions, i.e., by using the ground-state expressions $dW/dU_1 = N/2$ and $dW/dU_2 = -N^2/2$, as

$$|\mathbf{H}| = \frac{1}{2} \begin{vmatrix} dN/dU_1 & -dN^2/dU_1 \\ dN/dU_2 & -dN^2/dU_2 \end{vmatrix} = 0, \quad (8)$$

as required, for all U_1 and U_2 . This implies a vanish-

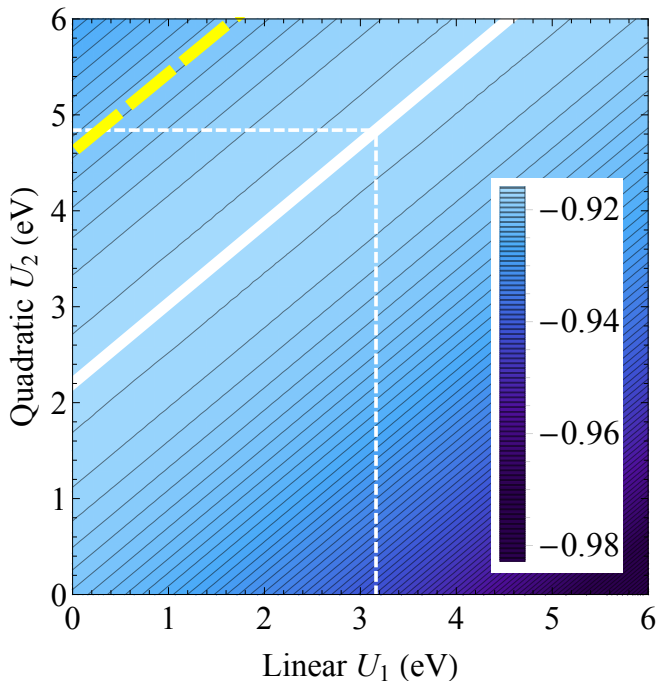


FIG. 3. (Color online) The constrained total-energy of stretched H_2^+ against the Lagrange multipliers U_1 and U_2 defined in Eq. 6. The subspace target occupancy is set to $N_c = N_{\text{exact}}$, and the zero is set to the exact total-energy. The constraint is satisfied at the total-energy maximum along the solid white line. The ionization potential is exact along the thick dashed line. The linear-response Hubbard U_2 , together with the U_1 value needed to correspondingly recover the exact subspace density, are shown using thin dashed lines.

ing energy curvature along the lines on which the corrective potential is constant. The linear-response Hubbard U at this bond length, calculated using a method adapted from Ref. 25, is 4.84 eV. If we intuitively set $U_2 = U$, then a corresponding $U_1 = 3.16$ eV is required to recover the exact subspace density. The line on which the ionization potential is exact (for the special case of H_2^+ , this means that the occupied Kohn-Sham state eigenvalue and the ion-ion energy sum to the exact total-energy, written $\varepsilon_{\text{DFT}} + E_{\text{ion-ion}} = E_{\text{exact}}$), intercepts $U_1 \approx 0$ eV at the linear-response $U_2 = U$, echoing the ‘SIC’ double-counting correction proposed in Ref. 47. Finally, for the constrained total-energy, we note that while it can be tuned to reach a maximum at the exact energy for a plausible target, $N_c = 0.511$ e, an unreasonable $U_1 = U_2 = -444.5$ eV is required to do so. We conclude, therefore, that an SIE affected ground-state cannot be systematically excited to a state that is less so by means of exact constraints, without breaking a physical symmetry. Put another way, the total-energy cannot typically be SIE-corrected by altering the density alone, and a non-vanishing energy correction term is required.

Such a correction is provided by the generalized DFT+ U term of Eq. 7, the total-energy generated by which is shown in Fig. 4. The zero of energy and the

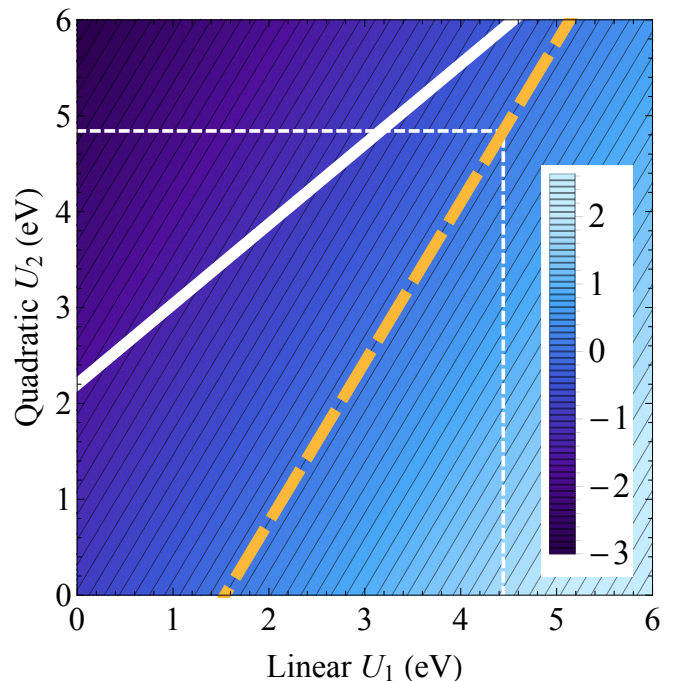


FIG. 4. (Color online) As per Fig. 3 but showing the free-energy obtained by setting $N_c = 0$ e in Eq. 6, i.e., using the generalized DFT+ U of Eq. 7. The thick dashed line is the exact energy intercept, and the thin dashed lines show the linear-response U_2 together with the corresponding U_1 needed to recover the exact energy. The solid white line, as in Fig. 3, indicates where the exact subspace occupancy is recovered.

heavy dashed line show E_{exact} , and the thin dashed lines indicate the Hubbard $U_2 = 4.84$ eV and corresponding $U_1 = 4.44$ eV required to recover it. E_{exact} is attained by a traditional DFT+ U calculation at $U_1 = U_2 = 3.85$ eV, and the intersection of the heavy solid and dashed lines yields the pair, $U_1 = 5.73$ eV and $U_2 = 6.98$ eV, at which E_{exact} and N_{exact} are located. At the same point, the Kohn-Sham eigenvalue ε_{DFT} lies at ~ 2.8 eV above $\varepsilon_{\text{exact}}$, reflecting that an accurate total-energy at a particular occupancy may coincide with an inaccurate ionization energy, and vice versa, as was recently shown in detailed analyses of the residual SIE in hybrid functionals⁴⁸ and in DFT+ U itself, at fractional total occupancies³².

The generalized DFT+ U functional enables simultaneous correction of the ionization potential and total-energy, or the correction of either together with Koopmans’ condition^{5,7,8}. In the one-electron case, as in H_2^+ , Koopmans’ condition may be enforced at $\varepsilon_{\text{exact}}$. The approximately parallel solid curves of Fig. 5 illustrate the large U_1 and U_2 values required to do so, as a function of internuclear distance. To estimate these, we have used the convenient feature of H_2^+ that the PBE $1s$ orbital subspace projectors closely match Kohn-Sham orbitals in spatial profile, almost exactly so at dissociation. As demonstrated by the occupancy curves in Fig. 5, this implies a negligible charge and kinetic self-

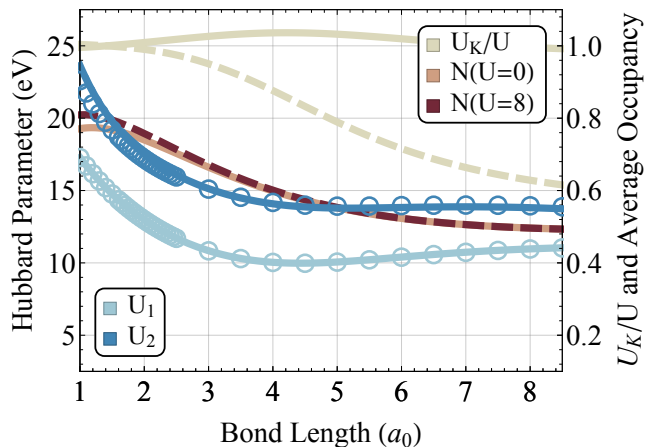


FIG. 5. (Color online) Generalized Hubbard U parameters estimated for the PBE H_2^+ molecule at varying bond lengths. Approximately parallel solid curves (blue, left) depict the U_1 and U_2 values required to recover the exact total-energy and Koopmans’ condition, assuming constant PBE subspace occupancies. Open circles show the corresponding quantities calculated using a practical scheme based on the conventional Hubbard U and the PBE occupied eigenvalue (see text). The topmost curves (sand, right) show the fraction of the latter U_1 (dashed) and U_2 (solid) due to the Koopmans term, U_K . On the same axis (dark red, right), we show that the average DFT+ U subspace occupancy is insensitive to the U value.

consistency effect, vanishing entirely for $U_1 = 2N_{\text{DFT}}U_2$, in subspace-uniform corrections such as those in question. For N_{sites} equivalent one-orbital subspaces spanning the energy window responsible for ε_{DFT} , the density non-self-consistent U_1 and U_2 are derived from $E_{\text{exact}} \approx E_{\text{DFT}} + N_{\text{sites}}(U_1N_{\text{DFT}} - U_2N_{\text{DFT}}^2)/2$, where $N_{\text{DFT}} = \text{Tr}[\hat{n}_{\text{DFT}}]$, and $\varepsilon_{\text{exact}} \approx \varepsilon_{\text{DFT}} + (U_1 - 2U_2N_{\text{DFT}})/2$, in which the subspace overlap and spillage are also neglected.

Since subspace response stiffening very typically results from the application of a conventional DFT+ U correction^{11,35}, it is promising to construct a charge non-self-consistent first-principles calculation scheme for U_1 and U_2 , e.g., for use in refining DFT+ U calculations in order to approximately enforce Koopmans’ condition. For this, let us suppose we have calculated a conventional U which reconciles the total energy reasonably, so that $E_{\text{exact}} \approx E_{\text{DFT}} + UN_{\text{sites}}(N_{\text{DFT}} - N_{\text{DFT}}^2)/2$. We may combine this with the previous two equations and a further requirement for Koopmans’ condition at an accurate energy, i.e., $\varepsilon_{\text{exact}} = E_{\text{DFT}}[N] - E_{\text{DFT}}[N - 1]$, where the latter is the DFT-estimated total-energy of the ionized system. This results (see Fig. 5 open circles for data) in

$$U_1 \approx U(1 - N_{\text{DFT}})(2 - N_{\text{sites}}N_{\text{DFT}}) + U_K, \quad \text{and} \\ N_{\text{DFT}}U_2 \approx U(1 - N_{\text{DFT}})(1 - N_{\text{sites}}N_{\text{DFT}}) + U_K, \quad (9)$$

where, with $U_K = 2(E_{\text{DFT}}[N - 1] - E_{\text{DFT}}[N] + \varepsilon_{\text{DFT}})$, we define the ‘Koopmans U ’. We emphasize that only convenient, approximate DFT quantities are used in

these formulae. The interdependence $U_1 - U_2N_{\text{DFT}} \approx U(1 - N_{\text{DFT}})$, for any value of N_{sites} , reveals the role of U in splitting U_1 and U_2 . In H_2^+ , Koopmans’ condition pushes both up to considerably higher values than are commonplace²⁸ for the conventional U of DFT+ U , which, following Ref. 32 and given N_{PBE} , lies close to its regime of minimal efficacy for eigenvalue correction. The Koopmans fraction of each parameter, U_K/U_1 or $U_K/(N_{\text{DFT}}U_2)$, generically denoted by ‘ U_K/U ’ in Fig. 5, lies close to unity for U_2 at all H_2^+ bond lengths, and it exceeds unity slightly when the U_K and U -related contributions tend to cancel. U_1 is also U_K -dominated at short bond lengths, at which $U_1 \approx N_{\text{DFT}}U_2$, before ultimately falling off to the average of U and U_2 in the fully dissociated limit. If the outlined proposed scheme is applied to finesse an existing DFT+ U calculation that is already accurate for recovering the total-energy, using a linear-response^{11,25} or otherwise calculated U , call it U_0 , then $U = 0$ eV is the appropriate value to use in our approximate formulae of Eq. 9. An approximately Koopmans’ compliant DFT+ U calculation then results from the use of the parameters $U_0 + U_K$ and $U_0 + U_K/N_{\text{DFT} + U_0}$, in place of U_1 and U_2 . The proposed scheme may be generalized to multi-orbital subspaces straightforwardly, in terms of the eigenvalues of \hat{n}_{DFT}^I instead of N_{DFT} . The constant- N_{DFT} approximation may be replaced by a linear-response approximation, in terms of χ , or lifted entirely by means of a parametrization of the occupancies and a numerical solution of the resulting equations.

To conclude, we have proven analytically, with stringent numerical tests, that non-linear constraints are incompatible with cDFT. It is not possible, therefore, to automate systematic SIE corrections of DFT+ U type by means of cDFT, notwithstanding the great utility of the latter, e.g., for correcting SIE by promoting broken symmetry, integer-occupancy configurations well described by approximate functionals^{10,42}. Nonetheless, we have found that the cDFT free-energy functionals, dubbed ‘generalized DFT+ U ’ functionals, offer the intriguing capability of simultaneously correcting two central quantities in DFT, the total-energy and the highest occupied orbital energy. Our approximate formulae for the required parameters, which may differ greatly from the familiar Hubbard U , offer a framework within which to further develop double-counting techniques and first-principles schemes for the promising class of SIE correcting methods based on DFT+ U ^{11,28,31,32}, as well as opening up possibilities for their diverse application. We envisage that SIE correction schemes of two or more parameters may also be useful for generalizing the exchange fraction of hybrid functionals⁴⁸, and for DFT+ U type corrections of perturbative many-body approximations such as GW ⁴⁹, the deviation from linearity of which is somewhat analogous to that of approximate DFT^{50,51}. For the analysis and correction of spuriously self-interacting multi-reference systems, we may learn much from the exact solution of minimal models⁵².

This work was enabled by the Royal Irish Academy –

Royal Society International Exchange Cost Share Programme (IE131505). GT acknowledges support from EPSRC UK (EP/I004483/1 and EP/K013610/1). GM and DDO'R wish to acknowledge support from the Science Foundation Ireland (SFI) funded centre AMBER

(SFI/12/RC/2278). All calculations were performed on the Lonsdale cluster maintained by the Trinity Centre for High Performance Computing. This cluster was funded through grants from Science Foundation Ireland.

* omuinneg@tcd.ie

- ¹ P. Hohenberg and W. Kohn, *Phys. Rev.* **136**, B864 (1964).
- ² W. Kohn and L. J. Sham, *Phys. Rev.* **140**, A1133 (1965).
- ³ R. O. Jones, *Rev. Mod. Phys.* **87**, 897 (2015).
- ⁴ A. Jain, Y. Shin, and K. A. Persson, *Nat. Rev. Mater.* **1**, 15004 (2016).
- ⁵ J. P. Perdew, R. G. Parr, M. Levy, and J. L. Balduz, *Phys. Rev. Lett.* **49**, 1691 (1982).
- ⁶ A. J. Cohen, P. Mori-Sánchez, and W. Yang, *Science* **321**, 792 (2008).
- ⁷ I. Dabo, A. Ferretti, N. Poilvert, Y. Li, N. Marzari, and M. Cococcioni, *Phys. Rev. B* **82**, 115121 (2010).
- ⁸ J. P. Perdew and A. Zunger, *Phys. Rev. B* **23**, 5048 (1981).
- ⁹ J. P. Perdew, K. Burke, and M. Ernzerhof, *Phys. Rev. Lett.* **77**, 3865 (1996).
- ¹⁰ B. Kaduk, T. Kowalczyk, and T. Van Voorhis, *Chem. Rev.* **112**, 321 (2012).
- ¹¹ H. J. Kulik, M. Cococcioni, D. A. Scherlis, and N. Marzari, *Phys. Rev. Lett.* **97**, 103001 (2006).
- ¹² A. J. Cohen, P. Mori-Sánchez, and W. Yang, *Chem. Rev.* **112**, 289 (2012).
- ¹³ A. Svane and O. Gunnarsson, *Phys. Rev. Lett.* **65**, 1148 (1990).
- ¹⁴ M. R. Pederson, A. Ruzsinszky, and J. P. Perdew, *J. Chem. Phys.* **140**, 121103 (2014).
- ¹⁵ T. Schmidt and S. Kümmel, *Phys. Rev. B* **93**, 165120 (2016).
- ¹⁶ D. Hofmann, S. Klüpfel, P. Klüpfel, and S. Kümmel, *Phys. Rev. A* **85**, 062514 (2012).
- ¹⁷ D. Hofmann, T. Körzdörfer, and S. Kümmel, *Phys. Rev. Lett.* **108**, 146401 (2012).
- ¹⁸ S. Klüpfel, P. Klüpfel, and H. Jónsson, *J. Chem. Phys.* **137**, 124102 (2012).
- ¹⁹ G. Borghi, A. Ferretti, N. L. Nguyen, I. Dabo, and N. Marzari, *Phys. Rev. B* **90**, 075135 (2014).
- ²⁰ V. I. Anisimov and O. Gunnarsson, *Phys. Rev. B* **43**, 7570 (1991).
- ²¹ V. I. Anisimov, J. Zaanen, and O. K. Andersen, *Phys. Rev. B* **44**, 943 (1991).
- ²² V. I. Anisimov, I. V. Solovyev, M. A. Korotin, M. T. Czyżyk, and G. A. Sawatzky, *Phys. Rev. B* **48**, 16929 (1993).
- ²³ S. L. Dudarev, G. A. Botton, S. Y. Savrasov, C. J. Humphreys, and A. P. Sutton, *Phys. Rev. B* **57**, 1505 (1998).
- ²⁴ W. E. Pickett, S. C. Erwin, and E. C. Ethridge, *Phys. Rev. B* **58**, 1201 (1998).
- ²⁵ M. Cococcioni and S. de Gironcoli, *Phys. Rev. B* **71**, 035105 (2005).
- ²⁶ D. J. Cole, D. D. O'Regan, and M. C. Payne, *J. Phys. Chem. Lett.* **3**, 1448 (2012).
- ²⁷ J. M. Garcia-Lastra, J. S. G. Myrdal, R. Christensen, K. S. Thygesen, and T. Vegge, *J. Phys. Chem. C* **117**, 5568 (2013).
- ²⁸ B. Himmetoglu, A. Floris, S. de Gironcoli, and M. Cococcioni, *Int. J. Quantum Chem.* **114**, 14 (2014).
- ²⁹ M. Setvin, C. Franchini, X. Hao, M. Schmid, A. Janotti, M. Kaltak, C. G. Van de Walle, G. Kresse, and U. Diebold, *Phys. Rev. Lett.* **113**, 086402 (2014).
- ³⁰ M. Shishkin and H. Sato, *Phys. Rev. B* **93**, 085135 (2016).
- ³¹ H. J. Kulik and N. Marzari, *J. Chem. Phys.* **133**, 114103 (2010).
- ³² Q. Zhao, E. I. Ioannidis, and H. J. Kulik, *J. Chem. Phys.* **145**, 054109 (2016).
- ³³ V. I. Anisimov, F. Aryasetiawan, and A. I. Lichtenstein, *J. Phys. Condens. Matter* **9**, 767 (1997).
- ³⁴ K. Nakamura, R. Arita, Y. Yoshimoto, and S. Tsuneyuki, *Phys. Rev. B* **74**, 235113 (2006).
- ³⁵ D. A. Scherlis, M. Cococcioni, P. Sit, and N. Marzari, *J. Phys. Chem. B* **111**, 7384 (2007).
- ³⁶ D. D. O'Regan, N. D. M. Hine, M. C. Payne, and A. A. Mostofi, *Phys. Rev. B* **82**, 081102 (2010).
- ³⁷ D. D. O'Regan, N. D. M. Hine, M. C. Payne, and A. A. Mostofi, *Phys. Rev. B* **85**, 085107 (2012).
- ³⁸ S. Curtarolo, G. L. W. Hart, M. B. Nardelli, N. Mingo, S. Sanvito, and O. Levy, *Nat. Mater.* **12**, 191 (2013).
- ³⁹ P. H. Dederichs, S. Blügel, R. Zeller, and H. Akai, *Phys. Rev. Lett.* **53**, 2512 (1984).
- ⁴⁰ P.-L. Sit, M. Cococcioni, and N. Marzari, *J. Electroanal. Chem.* **607**, 107 (2007).
- ⁴¹ D. D. O'Regan and G. Teobaldi, *Phys. Rev. B* **94**, 035159 (2016).
- ⁴² P. H.-L. Sit, M. Cococcioni, and N. Marzari, *Phys. Rev. Lett.* **97**, 028303 (2006).
- ⁴³ The DFT+*U* functionality³⁷ available in the ONETEP linear-scaling DFT package⁵³ was used with a hard (0.65 a_0 cutoff) norm-conserving pseudopotential⁵⁴, 10 a_0 Wannier function cutoff radii, and open boundary conditions⁵⁵.
- ⁴⁴ Q. Wu and T. Van Voorhis, *Phys. Rev. A* **72**, 024502 (2005).
- ⁴⁵ I. Dabo, *Towards first-principles electrochemistry*, Ph.D. thesis, Massachusetts Institute of Technology (2008).
- ⁴⁶ Total-derivatives are used here to indicate that self-consistent density response effects are included. The Hubbard parameters remain independent variables.
- ⁴⁷ D.-K. Seo, *Phys. Rev. B* **76**, 033102 (2007).
- ⁴⁸ V. Atalla, I. Y. Zhang, O. T. Hofmann, X. Ren, P. Rinke, and M. Scheffler, *Phys. Rev. B* **94**, 035140 (2016).
- ⁴⁹ H. Jiang, R. I. Gomez-Abal, P. Rinke, and M. Scheffler, *Phys. Rev. B* **82**, 045108 (2010).
- ⁵⁰ W. Nelson, P. Bokes, P. Rinke, and R. W. Godby, *Phys. Rev. A* **75**, 032505 (2007).
- ⁵¹ M. Dauth, F. Caruso, S. Kümmel, and P. Rinke, *Phys. Rev. B* **93**, 121115 (2016).
- ⁵² T. Olsen and K. S. Thygesen, *J. Chem. Phys.* **140**, 164116 (2014).
- ⁵³ C.-K. Skylaris, P. D. Haynes, A. A. Mostofi, and M. C. Payne, *J. Chem. Phys.* **122**, 084119 (2005).

⁵⁴ A. M. Rappe, K. M. Rabe, E. Kaxiras, and J. D. Joannopoulos, *Phys. Rev. B* **41**, 1227 (1990).

⁵⁵ G. J. Martyna and M. E. Tuckerman, *J. Chem. Phys.* **110**, 2810 (1999).